Relating Forest Biomass to SAR Data

T. Le Toan, A. Beaudoin, J. Riom, and D. Guyon

Abstract— **This paper presents the results of an experiment defined to demonstrate the use of radar to retrieve forest biomass. The SAR data were acquired by the NASA/JPL SAR over the Landes pine forest during the 1989 MAESTRO-1 campaign. The SAR data, after calibration, have been analyzed together with ground data collected on forest stands from young stage (8 yrs) to mature stage (46 yrs). The dynamic range of the radar backscatter intensity from forest was found maximum at *P*-band and decreases with increasing frequencies. Also, cross-polarized backscatter intensity yields the best sensitivities to variations of forest biomass. *L*-band data confirmed past results on good correlation with forest parameters. The most striking observation has been the strong correlation of *P*-band backscatter intensity to forest biomass. In order to develop algorithms to infer forest biomass from spaceborne SAR's, the experimental results will be compared with observations on other forest ecosystems and will be interpreted by theoretical modeling.**

I. Introduction

A major goal of the research in vegetation science is the development of an improved quantitative understanding of the state and dynamics of ecosystems and their interaction with the global cycles. A key to this understanding is the possibility of acquiring accurate measurements of the biophysical properties of the vegetation.

Today, one of the greatest uncertainties concerning the global carbon budget arises from a lack of information on forest biomass. The question of whether forests are a source or a sink of carbon is under discussion, partly because of the uptake of CO_2 from regenerating forests has not been studied extensively. Because regenerating vegetation accumulates carbon quickly during the first 20–30 yrs after disturbance, this is a critical period for accurate estimate of biomass and carbon storage [1], [2]. On the other hand, forests constitute a large portion of the Earth's renewable natural resources. All predictions indicate that demand for forest products will increase worldwide, while forested surfaces are continually decreasing. This statement highlights the need for an improved management of forest resources based on accurate, timely, and cost-effective forest volume inventories.

Remote sensing satellites have a considerable potential for monitoring forests on a regional or local scale. A number of studies have evaluated the utility of remote sensing data for mapping forest types and, to a lesser extent, for inferring forest stand parameters.

For optical sensors, vertical observations of the forest canopy are based on spectral reflectance data collected in visible and infrared regions. It is understood that the reflectance data of a tree is governed by the tree foliage properties, including the chlorophyll pigments, which absorb a large part of the incoming red radiation, the leaf angle orientation and the leaf internal structure, which affect the infrared radiation. For a forest canopy the reflectance data result from the foliage type, the crown area, and the understory vegetation or soil, especially when the canopy is not fully closed. When the tree types or species are known, forest stand parameters can be inferred from the crown area, which is related to parameters such as density, height, and biomass.

Franklin [3] reported that the visible reflectance of Landsat TM bands 1, 2, and 3 was strongly related to vegetation amount. Hame *et al.* [4] indicated a correlation coefficient $r^2 = 0.5$ for tree volume, mean diameter, and basal area with SPOT band 3 for conifers. Sader *et al.* [2] found that the Normalized Difference Vegetation Index (NDVI), which is the normalized ratio of red and infrared reflectance, he calculated from TM was sensitive to variations in the crown area and green biomass. However, the correlation between NDVI and the regeneration age is not very strong. De Wulf *et al.* [5] reported that stand density and average canopy height could be estimated from SPOT data. Still, the sensitivity of reflectance data to those forest parameters is no longer significant in canopies beyond 8 years old.

Despite the encouraging results obtained with optical data, at least with young forest stands, the use of the latter to retrieve forest stand parameters has not yet led to operational applications. The limitations concern, as a minimum, the following points: 1) it is intricate to retrieve parameters from mixed stands, 2) the sensitivity of reflectance data to forest parameters is not significant after the total coverage of the canopy, and 3) the disturbing effect of the understory vegetation has to be accounted for, in case of incomplete closure.

In recent years, there has been an increasing interest in the utility of radar data for forest ecosystem analysis. It was demonstrated that SAR data can be used to discriminate different forest types [6], and that the intensity in a SAR image at *L*-band is proportional to the aboveground biomass of the forest stands [7], [8].

With the present and forthcoming spaceborne imaging radar systems, namely ERS-1 in 1991, JERS-1 in 1992, and RADARSAT in 1994, there is a need for developing models and algorithms to incorporate the last findings into

Manuscript received June 1, 1991; revised September 26, 1991. The MAESTRO-1 campaign was supported and financed jointly by ESA and JRC. The conduct of the experiment was supported by the CNES and the French PNTS. The analysis work was performed under ESA Contract AO/1-2413/90/NL/PB.

T. Le Toan and A. Beaudoin are with the Centre d'Etude Spatiale des Rayonnements CNRS - Université Paul Sabatier Toulouse, France.

J. Riom and D. Guyon are with the Laboratoire de Bioclimatologie INRA Bordeaux, France.

IEEE Log Number 9105686.

more operational programs. The key questions concerning the possibility of inferring forest biomass from SAR data are the validity domains of the inversion algorithms regarding the SAR parameters, —frequency, polarization, incidence—, the forest type and growth stage, and the environment.

In order to observe and understand the relationships between SAR measurements and forest stand parameters, we conducted an experiment in the Landes forest, southwest France, during the 1989 MAESTRO-1 campaign. Compared to past experiments performed with an *L*-band SAR on the same test site, the 1989 campaign was focused on the possibility of having multifrequency (*P*-, *L*-, *C*- band) and polarimetric data together with an appropriate ground data collection plan, defined to collect relevant forest stand parameters.

This paper presents the results of data analysis, focusing on the relationships between measurements retrieved from SAR images and forest biophysical parameters.

II. The Experiment

The Joint Research Center (JRC) and the European Space Agency (ESA) have supported and financed the deployment of the NASA/JPL *C*-, *L*- and *P*-band polarimetric SAR in Europe in August 1989. The SAR was mounted on a NASA DC-8 aircraft. The campaign was called MAESTRO-1.

The deployment represented the first opportunity for European institutes to evaluate the ability of a multifrequency polarimetric SAR system to extract information of interest in forestry and agriculture. Four test sites have been selected for this campaign: Landes forest (France), Flevoland (The Netherlands), Thetford (UK), and Freiburg (Germany) [9].

This paper presents the experiment conducted at the Landes forest test site in France.

A. Test Site Description

In order to optimize the results obtained from the experiment, the test site has been selected to meet the following criteria: flat topography, homogeneous and large stands presenting an optimum range of forest parameters of interest. It is also understood that at this stage in research, monospecific stands will suit better as to increase our understanding of the mechanisms involving microwave interactions with vegetation canopies.

The Landes forest in southwestern France (near Bordeaux) is the largest plantation forest in France, constituting one million hectares on flat topography, producing 20% of the French timber. The forest is almost totally formed of maritime pine (*Pinus pinaster* (Ait.)) and is managed in a consistent fashion ensuring that the canopy is homogeneous. The test site selected for the experiment is an area of 7 km × 10 km comprising quasiuniform large stands of mean area of 25 hectares (~ 500 m × 500 m), rectangular in shape and delimited by fire protection tracks or access tracks.

Most of the stands are artificially sown, generally in rows of 4-m spacing; the rows following an east–west direction on the test site. The soils of the test site are podzols and show a large degree of heterogeneity. This heterogeneity is partly reflected by the natural understory vegetation.

The area includes many clear-cuts and a range of age classes from seedlings to stands over 46 years old. Consequently, these stands provide a wide range of forest parameters including density, diameter at breast height (dbh), tree height, and standing biomass. The test area, which has been utilized for previous remote sensing campaigns, represents a prototype of managed forest ecosystems, particularly appropriate for studies relating radar remote sensing data to forest parameters for the following reasons: 1) the stands are large and homogeneous, 2) the forest presents a relatively simple structure at the tree and stand level, this reduces the uncertainties in forest parameter measurements. In particular for microwave backscatter model, the complexity to derive model inputs is minimized, 3) the forest provides a wide range of forest parameters, especially in the range of interest (0–50 yrs) for radar data sensitivity study and for both ecosystem and forest management studies.

B. Ground Data Collection

The parameters selected for measurements are those that meet the requirements of both applications and modeling. Three types of ground data have been collected, accordingly to the methodologies specified in [10]:

1) *Forest inventory*: this involves the following description of the stand characteristics: stand age, management practices — sowing, thinning events — from data archive, row direction, crown cover, stand heterogeneity using air photography. Detailed observations have been made on forest stands, on sampling plot network used for many years. Six to 9 plots of 400 m^2 have been selected within each stand, where the following parameters have been measured: row spacing and width, tree density, dbh, tree height, canopy depth, natural understory species, cover, state, and height.

2) *Measurements performed during the radar overpass*: this includes data that vary rapidly with time: soil moisture, soil dielectric constant, moisture content of litter, undergrowth vegetation, and tree bark.

3) *Tree structure*: this involved detailed destructive measurements in order to determine the spatial distribution, the dimensions, and the moisture content of the various parts of the trees.

C. The SAR Data

The NASA/JPL airborne imaging radar system is a polarimetric SAR operating at *P*-band (0.44 GHz), *L*-band (1.225 GHz), and *C*-band (5.3 GHz) [11]. Three data lines were flown over the Landes forest on August 16, 1989. On the test area considered, two images acquired with orthogonal flight axis have been retained for analysis (look direction respectively perpendicular and parallel to row direction). The data provided are high resolution complex one-look product at *P*-, *L*- and *C*-band.

Fig. 1 presents a polarization color composite of the *P*-band image of the test-site, with a look direction perpendicular to row direction. HH, HV, and VV polarizations are respectively coded in blue, red, and green. A higher scaling factor has been applied to the red channel (HV), due to the data high dynamic range (~ 25dB) from HV to VV and HH. Rectangular forest

Fig. 1. *P*-band polarization color composite image of the Landes Forest test-site; HH, HV, and VV are respectively coded in blue, red, and green. The imaged area is approximately 9.5 km × 6.4 km, flight axis is up from right to left (east–west) and look direction is downward (perpendicular to row direction).

stands appear in color tones ranging from black and dark blue for clear-cut to bright white for mature forest (46 years old).

III. Data Analysis

A. SAR Data Quality

The data available from the MAESTRO-1 campaign were not calibrated. In order to analyze the backscatter intensity as a function of forest parameters retrieved from different forest stands located in the same image, within-image relative calibration in azimuth and across-swath must be achieved. For a given frequency, to intercompare intensity and phase between different polarization channels, adequate cross-talk removal, and channel balance in amplitude and phase is required. Finally, absolute calibration is needed for the joint analysis at different frequencies.

Overall radiometric quality of the JPL SAR data has been reported recently in [12]. In a long-term study, they concluded that the data was of good quality in term of long-term stability (stable absolute calibration), short-term stability (azimuth calibration), across-swath radiometric variations, and channel amplitude balance. However, they stressed out that the data should be calibrated particularly for: 1) cross talk at *L*-band, 2) channel imbalance at *P*-band, 3) phase imbalance at all frequencies, 4) across-swath radiometric variations at *P*-band, and 5) absolute calibration using given factors.

To assess and improve the data quality, an approach for external polarimetric calibration has been applied, using both extended targets of known properties and point targets deployed on the ground. During the SAR overpass, the following trihedral corner reflectors have been deployed: three trihedrals with 1.80-m sides, six trihedrals with 0.70-m sides and also eight with 0.44-m sides. Due to the lack of very low background backscatter, the smallest trihedrals have not been used in the analysis.

The overall calibration procedure applied to the data will be presented with more details in a separate study on polarimetric signatures of forest stands. It can be summarized in this paper as follows: The procedure is applied to unsymmetrized one look high resolution complex data. Cross-talk removal is performed using Klein's algorithm [13] while phase balance is performed using the approach formulated by Zebker and Lou [14] and Van Zyl [15]. Both corrections rely on backscatter statistics of clutter terrains, chosen to have azimuthal symmetry and uncorrelated cross- and copolarized scattering. Following, is the estimate of the amplitude of the channel imbalance terms using the ratio of copolarized terms from trihedral corner reflector backscatter. Due to the presence of significant background backscatter in the corner reflector vicinity, the trihedral response is estimated using the integrated approach [16], [17]. At the same time, absolute calibration factor is estimated from a comparison with the theoretical radar cross section of the trihedrals.

For the purpose of this paper, the quality assessment, before and after calibration, is evaluated as follows:

1) *within-image azimuth stability*: the SAR stability along the flight track was evaluated by comparing the radar backscattering coefficients retrieved from large identical fire protection tracks, located at different azimuths. In general, the data dispersion is less than 1 dB and no azimuthal correction needed to be applied;
2) *within-image across-swath radiometric variations*: reliable corner reflectors were deployed in a 25°–50° incidence angle ranges. At *L*-band, the response from the trihedrals was found to be quite stable, which was not the case at *P*-band as reported in [12]. It was not possible to conclude at *C*-band. Therefore, we restricted the imaged area to be analyzed in a limited range, from 40° to 50°.
3) *polarization channels balance*: the phase balance can be assessed by examining the trihedral scattering matrices. The raw phases between copolarized terms were found to be around 70°, 65°, and 130° at *P*-, *L*-, and *C*-band. After calibration, the copolarized (and cross polarized) terms are balanced within 10° (instead of 0° for an ideal trihedral). The amplitude imbalance before calibration was found to be significant at *P*-band, (2.5 dB) as reported in [12]. Therefore, calibration should have improved significantly the *P*-band amplitude balance, but it is difficult to assess due to the lack of extended target of known responses.
4) *absolute calibration*: the absolute calibration mean factors obtained from the trihedral analysis were in close agreement with the latest JPL correction factors [12], that is a difference in intensity of 0.6 dB at *P*-band, 0.54 dB at *L*-band, and 0.9 dB at *C*-band. These latest factors were used as they should provide a better absolute calibration.

B. Characterization of Pine Forest Biomass

For a given species, standing biomass is mainly a function of dbh, tree height, and stand density, which are themselves de-

pendent on tree age, forestry practices, and also environmental and genetic factors [18]. Generally, biomass can be estimated using one or more of the forest characteristics through the use of allometric equations.

For the Landes forest, the biophysical characterization of the pine stands has been done through existing allometric equations and also using simple models derived from field measurements. Environmental and genetic factors are not accounted for but can be neglected at this stage. Lemoine *et al.* [19] studied the growth and biomass of the maritime pine in the Landes forest and made intensive biomass measurements on 16-year-old trees. At the tree level, they found that the total weight W_c of each tree component type (needles, branch wood, trunk wood and trunk bark) was correlated to the trunk cross-sectional area C_s in square meters (directly related to the dbh). It was possible to estimate the weight of each tree component type through a simple relation:

$$W_c = a_0 C_s + a_1 \tag{1}$$

where c is a given component with its own coefficients a_0 and a_1. Then the total biomass at the stand level can be estimated by summing the different biomass contributions, knowing the mean C_s value within a given stand. However, it is expected that the coefficients vary with age, and this model should include other variables (such as tree height) to be generalized.

For other age classes, biomass estimates can also be realized using the measured biophysical parameters. Weight measurements were performed only on some trunks, but further experiments have been planned to study the crown biomass and relate it to standard parameters. Therefore, we will consider only the biomass contained in the trunks at this stage.

For the maritime pine, the trunks contain between 50 and 60% of the tree total standing biomass for a 16-year-old tree [19]. As the tree grows older, this fraction increases due to high self-pruning. Characterization of the trunk biomass is facilitated by the approximatively conical shape of the trunk. The trunk volume (m3) can be expressed in a first approximation as:

$$V_t = TC_sH = T\pi(dbh/2)^2H \tag{2}$$

where all dimensions are in meters, H is the tree height and T is a shape factor. At the stand level, the trunk volume V_{ts} (m^3/ha) can be estimated using:

$$V_{ts} = TsG\overline{H} \tag{3}$$

with

$$G = \overline{C_s}d_s = \pi(\overline{dbh}/2)^2 d_s$$

where G is the stand basal area (m^2/ha), d_s is the stand density, $\overline{H}$ is the stand mean height and T_s a stand shape coefficient. If we consider V_{ts} as being the trading timber volume (i.e., trunk including wood and bark), T_s has values around 0.45 for maritime pine [20]. We can consider T_s valid for all stands in a first approximation.

To obtain the trunk biomass, it is necessary to know the bark volume along with wood and bark density. For maritime pine over 20 years old, bark volume represents 25–30% of the total trunk volume [20]. If we consider this proportion constant with age, the stands trunk biomass can be estimated using:

$$W_{ts} = V_{ts}\overline{\rho_d} \tag{4}$$

where $\overline{\rho_d}$ is the mean dry wood density, including bark, found to be equal to 320 kg/m^3 from measurements.

This biomass estimation method is fairly simplified and probably lacks in precision, especially for young stands. However, estimates using (4) are in close agreement with those from (1), for stands around 16 years old.

At this time, complete compilation of forest parameters including trunk biomass is available for 24 stands which cover the range 8–46 years. However, there is a gap of measurements in the range 20–30 years. This is planned to be completed at a second test area.

The forest parameters of interest in this study are the following: canopy height, dbh, density, basal area, and trunk biomass.

The mean canopy height is estimated with an uncertainty varying from 0.2 to 1.2 m (95% confidence interval), giving a relative error of less than 5% for 2/3 of the stands and between 5 and 8% for the rest. The uncertainties associated with the density and basal area are higher due to sampling rate and to the estimates of sampling plot area: 7–14% for most of the stands. The trunk biomass of stands higher than 25 tons/ha has an uncertainty comparable to that of the basal area. For younger stands, the error is difficult to quantify.

Fig. 2 presents the data points for canopy height (m), dbh (cm), density (number of trees/ha), basal area (m^2/ha), and trunk biomass (tons/ha) as a function of age.

The forest parameters increase quasilinearly with age, except for basal area and stand density. Stand density is known to decrease exponentially due to thinning practices. Of particular importance for applications is the total trunk biomass which increases linearly with the stand age ($r^2 = 0.90$) without reaching a saturation level, for this range of age class from 0 to 46. The two circled data points are for two forest stands of 34 and 36 years, which are not representative. They are not included in the result of regression analysis between forest parameters given below, but are taken into account in the statistical studies of the relationships between backscatter coefficients and forest parameters.

Table I shows the correlation coefficients r^2 calculated from linear regression analysis between forest parameters of 22 forest stands, plus the point at the origin. In general, very high correlation coefficients are observed between most of the parameters, except between the basal area and the trunk density ($r^2 = 0.32$), trunk biomass and trunk density ($r^2 = 0.64$), and basal area and age ($r^2 = 0.66$). The age, height, dbh and trunk biomass are strongly intercorrelated ($r^2 >= 0.9$) while the trunk density and the basal area are not always good indicators of the general evolution, because of different thinning practices.

Nonlinear regression analysis was also performed between forest parameters and stand age, using exponential, logarithmic and power laws. Fig. 2 includes the best regression curves obtained from this analysis.

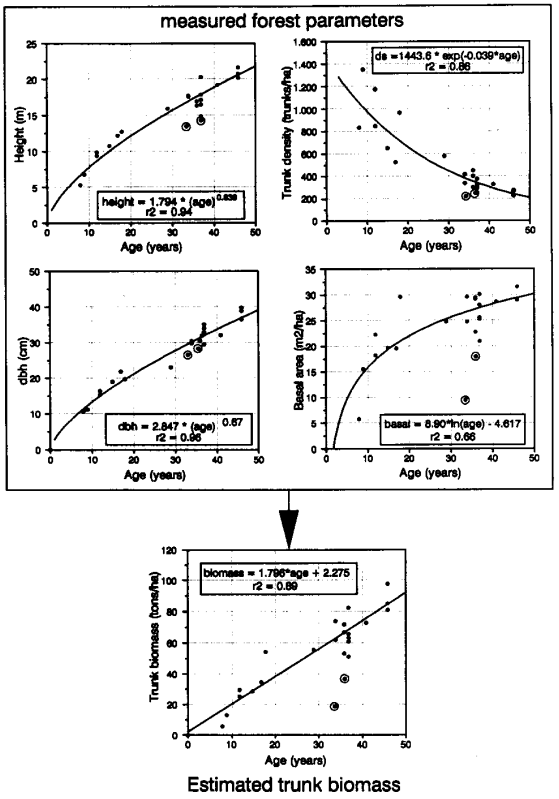

Fig. 2. Forest parameters as function of tree age.

TABLE I
CORRELATION COEFFICIENTS BETWEEN DIFFERENT FOREST BIOPHYSICAL PARAMETERS

CORRELATION COEFFICIENTS R^2 FROM LINEAR REGRESSION ANALYSIS BETWEEN FOREST PARAMETERS						
independent variable / dependent variable	AGE (years)	HEIGHT (m)	DBH (cm)	BASAL AREA (m2/ha)	LN DENSITY (trunks/ha)	TRUNK BIOMASS (tons/ha)
AGE (years)	1,00					
HEIGHT (m)		1,00				
DBH (cm)			1,00			
BASAL AREA (m2/ha)	0,66	0,78	0,72	1,00		
LN DENSITY (trunks/ha)	0,66	0,79		0,32	1,00	
TRUNK BIOMASS (tons/ha)			0,88	0,82	0,64	1,00

The previous results, obtained on the Landes forest, may indicate the general trend observed on this type of managed forests. However, any deviations from these trends should be due to local site conditions, historical conditions, and above all, forestry practices, which include thinning and fertilizing.

C. Forest Backscatter Dynamic Range

Backscattering coefficients related to forest stands from clear-cut to mature forest (46 years) are extracted from SAR data at *P*-, *L*-, *C*- band and at HH, VV, and HV polarizations. Then we define the forest backscatter dynamic range as the backscatter ratio between oldest forests and clear-cuts. Fig. 3 presents the forest backscatter dynamic range which decreases with the increasing frequency and decreases from HV to HH and VV. In this result at 45° incidence angle, the maximum ($\sim$ 15 dB) is observed at *P*-band HV, whereas only 2 dB are observed at *C*-band HH or VV.

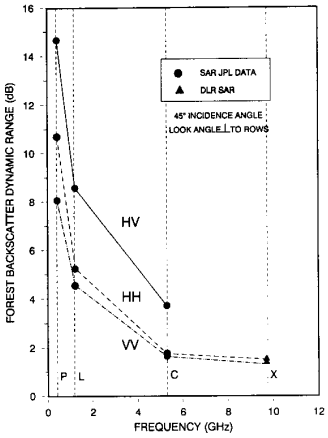

Fig. 3. Forest backscatter dynamic range in dB, as a function of polarization and frequency. The dynamic range is defined as $\sigma^\circ_{46\text{years}} / \sigma^\circ_{\text{clear-cut}}$ at *P*-, *L*-, and *C*-band, and $\sigma^\circ_{46\ \text{yrs}} / \sigma^\circ_{5\ \text{yrs}}$ at *X*-band.

In addition, SAR data acquired by the DLR SAR at *X*-band (HH and VV) on the same test site in July 1990 have been used. A dynamic range of 1–2 dB is measured at *X*-band over forest stands from 5 to 46 years, for both HH and VV polarizations.

The result presented here concerns a monospecific pine forest observed at 45° incidence. The observations indicate the general trend of the variation of dynamic range as a function of frequency and polarization. Values of dynamic range may vary according to forest types, incidence angles, and soil conditions.

D. Backscattering Coefficients as a Function of Forest Biomass

In this study, as we will focus on the relationships between the radar backscattering coefficients and the forest parameters, only *P*- and *L*-band data will be analyzed. The low sensitivity of backscattering coefficients measured at *C*- and *X*-bands to forest growth stage prevent us from a reliable analysis at these two last frequencies.

For regression analysis, together with the 24 stands for which all forest parameters are available, we included 9 clear-cut stands. For a total of 33 stands, the mean backscattering coefficients are related to each of the forest parameters. The mean backscattering coefficients in $(\mathrm{m}^2/\mathrm{m}^2)$ have been measured at *P*- and *L*-bands for HH, HV, and VV polarization, within the incidence angle range of 40–50°. The relatively large incidence range was necessary to incorporate the maximum number of stands in the analysis at the expense of higher data dispersion.

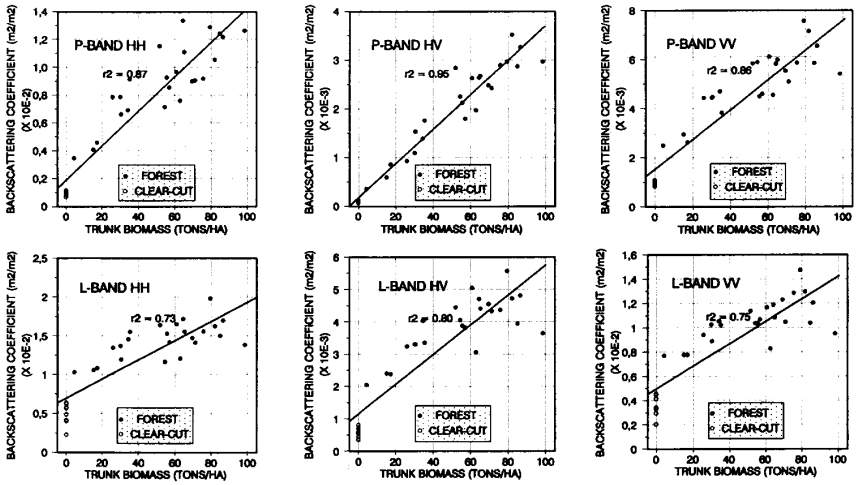

Fig. 4. Backscattering coefficients (natural units) at P- and L-band and HH, HV, and VV polarizations as functions of the trunk biomass at the stand level.

TABLE II
CORRELATION COEFFICIENTS BETWEEN L- AND P-BAND, HH, HV, AND VV BACKSCATTERING COEFFICIENTS AND FOREST PARAMETERS

CORRELATION COEFFICIENTS R^2 FROM LINEAR REGRESSION ANALYSIS BACKSCATTER AS A FUNCTION OF FOREST PARAMETERS	AGE (years)	HEIGHT (m)	DBH (cm)	BASAL AREA (m2/ha)	DENSITY (trunks/ha)	TRUNK BIOMASS (tons/ha)
L-BAND HH	0,78	0,85	0,85	0,83	0,32	0,73
L-BAND HV	0,77	0,87	0,84		0,23	0,80
L-BAND VV	0,73	0,83	0,79	0,86	0,16	0,75
P-BAND HH	0,87			0,88	0,39	0,87
P-BAND HV	0,87		0,89	0,87	0,43	
P-BAND VV	0,76	0,86	0,83		0,18	0,86

Table II includes the correlation coefficients r^2 obtained by taking each of the forest parameters as an independent variable. An excellent correlation is found with height, biomass, dbh, basal area, and age in decreasing order, and no significant correlation is found with the tree density. In general, the correlation coefficients are higher with P-band compared to L-band. HH and VV yield similar correlations with a slight advantage for HH. The best correlation coefficient has been obtained between P-band and HV and the trunk biomass ($r^2 = 0.95$).

Fig. 4 shows the backscattering coefficients as a function of the estimated total trunk biomass at the stand level for L-band and P-band and at HH, HV, and VV polarizations. The data dispersion, caused by factors including the uncertainties in biomass estimates and within-image across-swath variations, should be reduced if we could restrict the incidence angle range. An interesting observation concerns the fact that no saturation seems to occur within the biomass range (5–99 tons/hectare).

At all frequencies, the best sensitivity of σ° to trunk biomass is observed for cross-polarized returns. (Note that different scales of σ° have been used in Fig. 4). Also, P-band data have the highest sensitivity. Fig. 5 presents the backscattering coefficients in dB at P-band as a function of trunk biomass in tons/hectare, in log scale, for forests from 8 to 46 yrs.

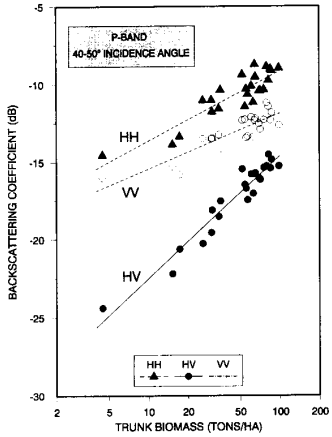

Fig. 5. Backscattering coefficients (in dB) at P-band, HH, HV, and VV, as functions of trunk biomass (in logarithmic scale) for forest from 8 to 46 years.

E. Polarization Phase Difference

An important radar backscattering information is the polarization phase difference (PPD) between the HH and VV polarizations. In this paper, the phase calibration performed on the SAR data set allowed the derivation of an absolute PPD, which is given by:

$$\Delta\Phi = \Phi_{HH} - \Phi_{VV} = \arg(S_{HH} * S^*_{VV}) \qquad (5)$$

where S_{HH} and S_{VV} are the HH and VV complex scattering coefficients and * denotes complex conjugate. We estimated that the PPD was slightly overestimated by approximately 7°. Then the incoherent mean and standard deviation of the PPD is calculated for the 33 forest stands.

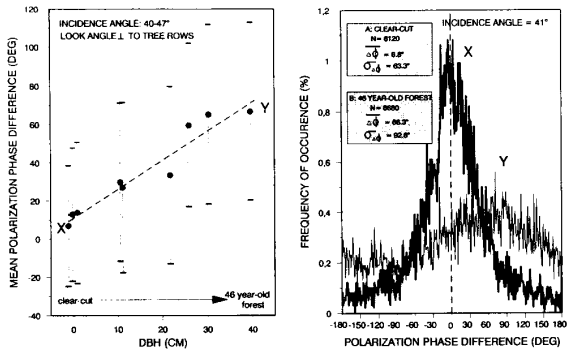

Fig. 6. (a) *P*-band mean polarization phase difference between HH and VV polarizations as a function of dbh, at an incidence angle range from 40 to 47°. (b) Polarization phase difference histograms of a clear-cut and a 46-year-old forest (point X & Y in Fig. 6(a)).

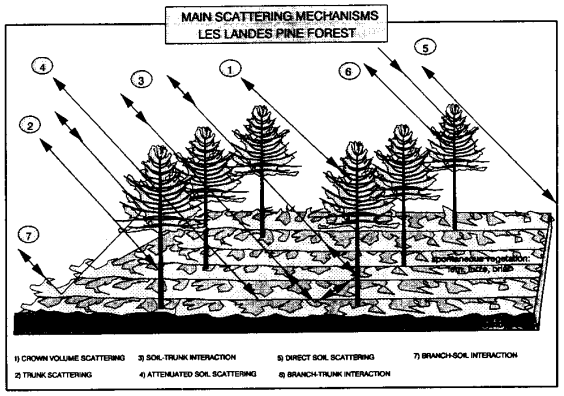

Fig. 7. Schematic view of the main scattering mechanisms in a forest canopy.

The PPD of vegetation with dominant vertical structure was found to be different from that of bare fields or fields covered with other vegetation [21], [22]. Since the PPD of fields constituted of vertical cylinders was found sensitive to cylinder number density, diameter, and dielectric constant, PPD of forest stands at *P*-band was analyzed as a function of forest parameters. As the PPD can be highly sensitive to the incidence angle [21], observations were made in a limited range of incidence. Notice that for the PPD analysis, we used the image acquired with a look direction perpendicular to row direction.

Fig. 6(a) shows the *P*-band mean PPD values as a function of dbh, for 9 forest stands at incidence angles from 40 to 47°. The mean PPD increases from 10 for a clear-cut to around 65° for 46-year-old forests. The PPD standard deviation is large, about 70° for clear-cut, up to more than 90° for forest stands. High correlation was found between mean PPD and dbh, but mean PPD was found also significantly related in decreasing order to stand age, height, trunk biomass and basal area.

Fig. 6(b) shows the PPD histograms of a clear-cut and a 46-year-old forest (point X & Y of Fig. 6(a)). For point X, the PPD exhibits a distribution centered near 0°, which was observed for similar surfaces in [21]. On the opposite, the PPD distribution of point Y has a broader distribution with a mean value of about 65°. Forests with age in the 0–46 year range exhibits PPD distribution in between these two distributions.

IV. Interpretation

The experimental results obtained on the Landes forest show obvious usefulness of *L*- and especially *P*-band radar for retrieving forest biomass. At present, cross comparison with observations on other forest sites and validation of observations by physical modeling are a requisite to the development of application programs.

From the results on correlation coefficients, it is not obvious to conclude about the particular effect of a given forest parameter, since those parameters are highly intercorrelated. However, the set of observations can provide useful indications to initiate the modeling phase.

In recent years, several authors have investigated the scattering mechanisms of forest based on observations [23]–[25]. Most of the descriptions were given for a single frequency case. In the following, we attempt to give a schematic view at different frequencies.

Fig. 7 illustrates scattering mechanisms that can be identified: backscatter from the crown volume (1), backscatter from trunks (2), double-bounce scattering from trunk and ground (3), backscatter from ground attenuated by the canopy (4), and directly from bare ground (5), multiple branch scattering (6) and branch-ground scattering (7). On the other hand, direct contribution from the bare ground may not be present in this forest observed at 45° of incidence (no gap, row interval 4 m, tree interval in row 3–4 m, height of the forest mostly >6 m). Also, the direct backscattering from the vertical trunks may not be significant at 45°. Reversely, the understory vegetation may have a contribution and it is possible that multiple scattering between the different elements have to be accounted for. The magnitude of the scattering terms and their relative importance depend, for a given forest type, on the tree growth stage and on radar parameters—polarization, incidence, and above all, frequency.

At *X*-band, the sources of scattering are twigs and needles from the upper part ($\sim$ 1m) of the crown. In this case of coniferous forest, the tree growth follows a given architecture model and the ideal architecture is repeated every year at the top of the trees ([26]). As different forest stands from young to mature stage have similar tree top structure, the low dynamic range of the related *X*-band radar backscattering coefficients can be easily understood.

At *C*-band, the sources of scattering should be located within a deeper crown volume. However, we expect that the penetration will not exceed the crown thickness in most cases. It is to be noted that the crown thickness increases with tree age during the young growth stage, and becomes stable at about 7 m, beyond 15–17 yrs. Also, it was found that the HH and VV radar backscattering coefficients reach a stability value after 10 yrs (about -8.5 dB at 45° of incidence). These observations explain the relatively low dynamic range of *C*-band backscatter of the monospecific stands under study. Within the crown volume, the scattering mechanisms include

the direct scattering from the crown elements and the multiple scattering between crown elements: foliage, branch, trunk, with certainly a minor contribution of the foliage (twigs and needles) at this frequency.

At L-band, the penetration depth exceeds the crown layer and mechanisms involving the lower part of the canopy must be present. The most important scattering processes should be: a) direct backscatter from the crown layer (mostly branches), b) double scattering from the tree trunk to the ground, this component is two-way attenuated by the crown layer, c) backscatter from the ground surface also attenuated twice, as it propagates through the crown and trunk layers. The relative importance of the scattering terms must be specified by modeling results. However, experimental results show that: a) the highest correlation has been observed with the basal area for all polarizations and b) cross-polarization data are more correlated to basal area and other forest parameters than HH and VV data. The best correlation coefficient at L-band is between HV and basal area ($r^2 = 0.91$).

At this stage, we understand that the L-band backscatter should result from major contribution of the crown layer (mainly branches) and contribution of the trunk. An interesting experimental result from [19] concerns the basal area that was found to be the best estimator of the total above ground biomass, including branch biomass, leaves biomass, and trunk biomass, each component being strongly correlated to the basal area.

At P-band, all the scattering mechanisms identified at L-band should be present. The observations at this frequency can be summarized as follows:

1) very high correlation coefficients have been observed with height, trunk biomass, dbh, basal area in this decreasing order;
2) cross-polarized returns have higher correlation coefficients with forest parameters;
3) VV returns are lower than HH, about 2–3 dB. HV returns have relatively high values (~ -15 dB) at high forest biomass values and low returns at low biomass (~ -25 dB);
4) the mean polarization phase difference between HH and VV increases with stand age and forest parameters, reaching 50–60° values for oldest stands.

Since a strong correlation of the radar backscatter intensity to trunk biomass has been observed, one may suspect that the tree trunk should have the major contribution to the radar backscatter. However, if the trunk–ground interaction is the dominant mechanism encountered, the dihedral corner reflector effect should yield 1) very low or insignificant cross-polarized returns and 2) high polarization phase difference (180° for a perfect dihedral). This was not observed. In this case, only modeling approach, based on observations, will enable us to identify the relevant scattering mechanisms.

V. Conclusions and Future Works

This study has demonstrated experimentally the use of SAR data to retrieve forest parameters, in particular, the forest biomass ,which is of prime importance in ecosystem studies and in forest management applications.

Using multifrequency SAR data, the results confirm past findings on the possibility to infer the forest above ground biomass from L-band data. But the most striking observations have been obtained with P-band data, which have the strongest correlation and the highest sensitivity with forest biomass. Also cross-polarized backscatter intensity yields the best results in terms of forest biomass retrieval.

Before incorporating the above findings in operational applications, and also in order to define optimum SAR's for future remote sensing missions, further works have to performed, which includes the following:

1) The results have to be intercompared with observations performed on other forest ecosystems. At first, the results obtained on the Landes Forest (Maritime Pine) will be compared to observations at other coniferous forests (e.g., Loblolly Pine at Duke Forest). In a next step, different forest types (e.g., deciduous species, mixed stands) and ecosystems environments (e.g., tropical forest) will be considered;
2) The measurements must be validated by physical modeling developed based on the observations. Multifrequency polarimetric data present in this case the optimum data set for model development. Simulation studies using validated models will then be used to assess the sensitivity and the robustness of algorithms developed to retrieve forest biomass from various forest ecosystems.

However, at this stage in research, the results already show one of the most encouraging issues in using remote sensing to monitor the Earth's ecosystems.

Acknowledgment

The authors would like to thank particularly the MAESTRO-1 campaign managers, Peter N. Churchill (JRC) and Evert P.W. Attema (ESA).

References

[1] S. Brown, "Rates of organic matter accumulation and litter production in tropical forest ecosystems," in *The Role of Tropical Forests on the World Carbon Cycle*, S. Brown, A. E. Lugo, and B. Liegel, Eds. Springfield, VA: NTIS, pp. 118–139, 1980.

[2] S. A. Sader, R. B. Waide, W. T. Lawrence, and A. T. Joyce, "Tropical forest biomass and successional age class relationships to a Vegetation Index derived from Landsat TM data," *Remote Sensing of the Environment*, vol. 28, pp. 143–156, 1989.

[3] J. Franklin, "Thematic Mapper analysis of coniferous structure and composition," *Int. J. Remote Sensing*, vol. 7, pp. 1287–1301, 1986.

[4] T. Hame, F. Tompo, and E. Parmes, "Stand-based forest inventory from SPOT image," in *Proceedings Symposium SPOT-1 Image Utilisation, Assessment, Results*. Toulouse: CNES, pp. 971–976, 1988.

[5] R. R. DeWulf, R. E. Goossens, B. P. DeRoover, and F. C. Borry "Extraction of forest stand parameters from panchromatic and multispectral SPOT-1 data," *Int. J. Remote Sensing*, vol. 11, no. 9., pp. 1571–1588, 1990.

[6] J. Cimino, A. Brandani, D. Casey, J. Rabassa, and S. D. Wall "Multiple incidence angle SIR-b experiment over Argentina: Mapping of forest units," *IEEE Trans. Geosci. Remote Sensing*, vol. GE-24, pp. 498–509, 1986.

[7] J. Riom and T. Le Toan, "Relations entre des types de forets de pins maritimes et la rétrodiffusion radar en bande L", in *Proc. of Spectral Signatures of Objects in Remote Sensing Symp.*, Avignon, France, pp. 455–465, 1981.

[8] S. T. Wu, "Potential application of multipolarization SAR for pine-plantation biomass estimation," *IEEE Trans. Geosci. Remote Sensing*, vol. GE-25, no. 3, pp. 403–409, 1987.
[9] P. N. Churchill and E. P. W. Attema, "MAESTRO-1 Campaign 1989, experiment plan," Joint Rep. of the JRC Institute for Remote Sensing Applications, Ispra (Italy) and ESA/ESTEC, Noordwijk (The Netherlands), July 1989.
[10] P. N. Churchill, "Procedures for the collection and compilation of forest ground data in microwave experiments," Tech. Note, JRC Institute for Remote Sensing Applications, Ispra, Italy, 1989.
[11] D. N. Held *et al.*, "The NASA/JPL multifrequency, multipolarization airborne SAR system," Proc. of IGARSS'88 Symp., Edinburgh, Scotland, pp. 317–322, 1988.
[12] A. Freeman, Y. Shen, J. Van Zyl, and J. D. Klein, "Calibration of NASA/JPL DC-8 SAR data," in Proc. IGARSS'91 Symp., Helsinki, Finland, vol. 3, pp. 1377–1379, 1991.
[13] J. D. Klein and A. Freeman, "Quadpolarization SAR calibration using target reciprocity," *J. Electr. Waves and Appl.*, vol. 5, no.7, pp. 735–751, 1991.
[14] H. A. Zebker and Y. Lou, "Phase calibration of imaging radar polarimeter Stokes matrices," *IEEE Trans. Geosci. Remote Sensing*, vol. 28, pp. 246–252, 1990.
[15] J. Van Zyl, "Calibration of polarimetric radar images using only image parameters and trihedral corner reflector responses," *IEEE Trans. Geosci. Remote Sensing*, vol. 28, pp. 327–348, 1990.
[16] R. Touzi, "Analyse d'images radar en Télédétection: améliorations radiométriques, filtrage du speckle et détection de contours," Thèse de Doctorat, Université Paul Sabatier, Toulouse, 1988.
[17] A. L. Gray, P. W. Vachon, C. E. Livingstone, and T. I. Lukowski, "Synthetic Aperture Radar calibration using reference reflectors," *IEEE. Trans. Geosci. Remote Sensing*, vol. 28, pp. 374–383, 1990.
[18] E. S Kashischke and N. L. Christensen, "Connecting forest ecosystem and microwave backscatter models," *Int. J. Remote Sensing,* vol. 11, no. 7, pp. 1277–1298, 1990.
[19] B. Lemoine, J. Gelpe, J. Ranger, and C. Nys, "Biomasses et croissance du pin maritime. Etude de la variabilité dans un peuplement de 16 ans," *Ann. Sci. For.*, vol. 43, no. 1, pp. 67–84, 1986.
[20] B. Lemoine and N. Decourt, "Tables de production pour le pin maritime dans le sud ouest de la France," *R. F. F. XXI*, vol. 1, pp. 5–16, 1969.
[21] F. T. Ulaby, D. Held, M. C. Dobson, K. C. Mc Donald, and T. B. A. Senior, "Relating polarization phase difference of SAR signals to scene properties," *IEEE Trans. Geosci. Remote Sensing*, vol. GE-25, pp. 83–91, 1987.
[22] J. R. Wang and T. Mo, "The polarization phase difference of orchard trees," *Int. J. Remote Sensing*, vol. 11, no. 7, pp. 1255–1265.
[23] J. A. Richard, G. Q. Sun, and D. S. Simonett, "*L*-band radar backscatter modeling of forest stand," *IEEE Trans. Geosci. Remote Sensing*, vol. GE-25, pp. 487–498, 1987.
[24] S. L. Durden, J. Van Zyl, and H. A. Zebker, "Modeling and observation of radar polarization signature of forested areas," *IEEE Trans. Geosci. Remote Sensing*, vol. 27, pp. 290–301, 1989.
[25] F. T. Ulaby, K. Sarabandi, K. McDonald, M. Whitt, and M. C. Dobson "Michigan Microwave Scattering Model," *Int. J. Remote Sensing*, vol. 11, no.7, pp. 1223–1253, 1990.
[26] E. Mougin, T. Le Toan, A. Lopes, P. Borderies, and A. Sarremejean, "Backscattering measurements at *X*-band on young coniferous trees," in *Proceedings of IGARSS'87 Symposium,* Ann Arbor, MI, pp. 287–292, 1987.

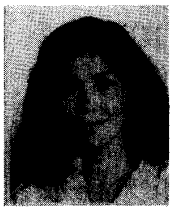

Thuy Le Toan received the Engineer degree and the Ph.D. degree in physics from the Paul Sabatier University, Toulouse, France. In 1973, she joined the Centre d'Etude Spatiale des Rayonnements.

Since 1980, her research activity has been in the area of microwave remote sensing applied to vegetation. Her research interests include experimentation and modeling of microwave interaction with agricultural and forested media, and analysis of SAR images. She has served as the Project Coordinator and Principal Investigator of several microwave airborne experiments in Europe and is the Principal Investigator of ERS-1 and SIR-C project.

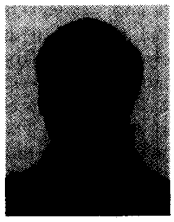

A. Beaudoin received the B.S. degree and the M.S. degree in physical geography in 1986 and 1989, respectively, from the Université de Sherbrooke, Québec, Canada. He is currently working toward the Ph. D. degree in physics, specializing in microwave remote sensing, at the Université Paul Sabatier, Toulouse, France.

His current research interests include microwave remote sensing applied to vegetation and terrestrial ecosystems, using modeling approaches for the development of algorithms devoted to applications such as forest and land-use mapping and retrieval of vegetation biophysical parameters.

J. Riom is a research scientist in the Remote Sensing and Forestry Research Unit Laboratory of Bioclimatology, Institut National de la Recherche Agronomique, Bordeaux, France. His research interests include applications of remote sensing data (SPOT, Landsat TM, radar, aerial photographs) to forest monitoring and forest inventory purposes.

D. Guyon is a research engineer in the Remote Sensing and Forestry Research Unit, Laboratory of Bioclimatology, Institut National de la Recherche Agronomique, Bordeaux, France. Her research field includes the characterization of structural parameters of maritime pine stands using visible, near infrared, middle infrared (SPOT, Lansat TM) and radar remote sensing data.